Incorporating ground cracks in the estimation of post-seismic landslide susceptibility

Shui Yamaguchi, Mio Kasai[§],
Research Faculty of Agriculture
Hokkaido University
Kit-9, Nishi-9, Kita-ku, Sapporo, Japan
[§]kasaim@for.agr.hokudai.ac.jp

Abstract—**An intense earthquake not only induces numerous landslides over a broad area, but can also trigger landslides; this is because the ground loses strength when strong tremors occur. Following an earthquake, landslide susceptibility should be appraised immediately to avoid further disasters and enable safe and prompt restoration work to proceed in the affected region. This study developed a topographic index to represent a soil mass with dense seismic ground cracks (DCI), to allow the degree of ground disturbance to be expressed on a local scale. The index was then used as a conditioning factor in a statistical model based on the weight of evidence (WoE) approach, to assess the correlation between DCI and landslides and estimate landslide susceptibility. An analysis of 38 post-seismic slides was conducted in a 2 km^2 area of the Aso region in Kyushu, Japan, where a powerful earthquake (Mw 7.0) struck in April 2016. Tectonic, seismic, lithological, climatic, and vegetational conditions were assumed to be similar over the area due to its small size, and only topographic conditioning factors were considered. The results demonstrated a correlation between DCI and post-seismic landslide occurrence, and the area under the receiver operating characteristic curve (AUC) indicated slightly greater model accuracy when DCI was included. Further studies using larger datasets are required to develop an appropriate model to express the relationships between the index and controlling factors, to improve the accuracy of post-seismic slide susceptibility assessments.**

I. INTRODUCTION

An intense earthquake can trigger numerous landslides over a broad area, causing damage to human lives, property, and infrastructure. Following an earthquake, an area will remain prone to landslides because ground that is affected by strong tremors requires months to years to recover its strength. Under these circumstances, landslide susceptibility should be appraised as soon as possible to avoid further disasters and enable safe and prompt restoration work to begin in the area. Appraisals are often made by the "direct method" [1], i.e., identifying topographic features indicative of slope instability, such as ground cracks, slope knick lines, and steep slopes, via field survey and/or examining aerial photographs or topographic maps derived from a light detection and ranging (LiDAR) survey. However, this is time-consuming and labor-intensive work, and the outcome can vary according to the skill of the operators. As an alternative, landslide susceptibility can also be estimated indirectly using a statistical model incorporating tectonic, lithological, climatic, hydrologic, topographic, and vegetation conditioning factors [2]. This method has been widely applied to co-seismic slides [3,4,5], while it has rarely been used for post-seismic slides, possibly because of a shortage of information regarding landslides after an intense earthquake. An appropriate and accurate model for post-seismic slides would facilitate assessments of landslide susceptibility over a broad area.

In this study, we attempted to develop a statistical model to appraise post-seismic landslide susceptibility by considering seismic ground cracks. The location of the ground cracks is a key issue when using the direct method, but is rarely considered in statistical models, due to the coarse resolution of elevation data and the difficulty of digital expression of the features. A 2 km^2 area of the Aso region in Kyushu, Japan, where a powerful earthquake (Mw 7.0) occurred in April 2016, was selected for the analysis (Figure 1). As the first step, an index to represent soil mass with dense seismic ground cracks (DCI) was proposed by employing a surface roughness filter. The DCI, together with topographic factors selected following a field survey [6], was then assessed using the weight of evidence (WoE) approach [7], to examine the correlation between the indices and the occurrence of landslides, and estimate landslide susceptibility. Finally, landslide susceptibility estimations were compared with versus without use of the DCI, to determine the improvement in the model achieved by incorporating seismic ground cracks into the set of conditioning factors.

Shui Yamaguchi and Mio Kasai (2020) Incorporating ground cracks in the estimation of post-seismic landslide susceptibility:
in Massimiliano Alvioli, Ivan Marchesini, Laura Melelli & Peter Guth, eds., Proceedings of the Geomorphometry 2020 Conference, doi:10.30437/GEOMORPHOMETRY2020_45.

II. STUDY AREA

The study area was located on a flank of the caldera wall of the Aso volcano, underlain by Middle Pleistocene pyroxene, andesite, and pyroclastic rock. The 2016 earthquake caused 76 slides and numerous cracks over an area of 2 km^2. A further 38 landslides were later induced by rainfall; these were of the shallow translational type, and some of them yielded a debris flow. Landslides increased in size continuously following the earthquake; this phenomenon was not accounted for in this study. A landslide inventory was compiled based on aerial photographs and LiDAR survey data acquired simultaneously in January 2015, and in April and August 2016. Slopes where landslides were initiated were targeted for the analysis; therefore, sediment transfer and deposition zones were not included in the inventory. Tectonic, seismic (e.g. peak ground acceleration), lithological, and climatic conditions were presumed to be equal throughout the study area due to its small size. The entire area was covered with aged *Cyptomeria japonica*.

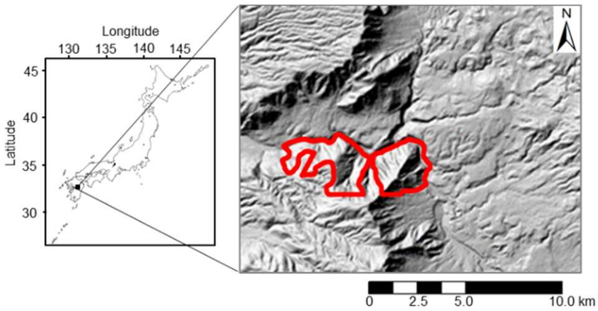

Figure 1. Study area (outlined in red)

III. METHODS

The DCI was derived from a surface roughness filter, based on the assumption that crack formation is associated with an increase in roughness. In this study, we applied a standard deviation of a slope angle for 3 × 3 cells, σ_s, proposed by [8], to the filter, using a 1-m digital elevation model (DEM). We assumed that cracks appeared in cells where the change in standard deviation from pre- (January 2013) to post- (April 2016) earthquake conditions ($\sigma_{s\ chg}$) was greater than or equal to a threshold value (C_m). The change was calculated as follows:

$$\sigma_{s\ chg} = \sigma_{s\ post} - \sigma_{s\ pre} \qquad (1)$$

where the subscript indicates the timing of the LiDAR survey used to produce two DEMs. We compared the spatial distributions of $\sigma_{s\ chg}$ and seismic ground cracks identified in the field, or based on topographic maps generated after the earthquake, to determine C_m. Then, cells with $\sigma_{s\ chg} \geq C_m$ were converted into points to calculate the point density using a kernel density function with a bandwidth of 10 m for each 1-m cell in the ArcGIS software environment. The density was defined as DCI.

The WoE method [7] was applied to estimate the susceptibility to post-seismic landslides. A bivariate model was used to examine the correlation between DCI and the occurrence of post-seismic landslides. We randomly selected 68% of the landslides (26) to train the model; the remaining 12 were used for testing. The correlation between a certain conditioning factor class and landslides is given by the contrast, C, as follows:

$$C = W^+ - W^- \qquad (2)$$

where W^+ is the positive weight of evidence for a certain conditioning factor class, and W^- is the negative weight of evidence for the class for a 1-m cell. They are given by:

$$W^+ = \ln \frac{P(F|L)}{P(F|\overline{L})} \qquad (3)$$

$$W^- = \ln \frac{P(\overline{F}|L)}{P(\overline{F}|\overline{L})} \qquad (4)$$

where L indicates the presence of a landslide, F indicates the presence of a value within a certain conditioning factor class, $\overline{L}$ indicates the absence of a landslide, $\overline{F}$ indicates the absence of a value within a certain conditioning factor class, $P(F|L)$ is the probability of a 1-m landslide cell conditioning a value within a certain conditioning factor class, $P(F|\overline{L})$ is the probability of a cell outside of a landslide containing a value within a certain conditioning factor class, $P(\overline{F}|L)$ is the probability of a 1-m landslide cell not containing a value within a certain conditioning factor class, and $P(\overline{F}|\overline{L})$ is the probability of a cell outside of a landslide not containing a value within a certain conditioning factor class. The combination of positive W^+ and negative W^-, or high C, suggests a positive relationship between landslide occurrence and that conditioning factor class. In contrast, a combination of negative W^+ and positive W^- indicates a negative relationship. If landslide occurrence is independent of the factor class, then W^+ and W^- both equal 0. The classes of DCI and other conditioning factors, slope angle, plan and profile curvature, and topographic wetness index (TWI) obtained for each 1-m cell are shown in Table 1. The plan and profile curvature values for each cell provided excessively detailed topographic information, and appeared not to show the effects of slope profiles on landslide occurrence appropriately. Therefore, we averaged these values within a 10-m radius of each cell, as described previously by [9], and incorporated the results into the model. The variance inflation factor (VIF) of the included factors ranged from

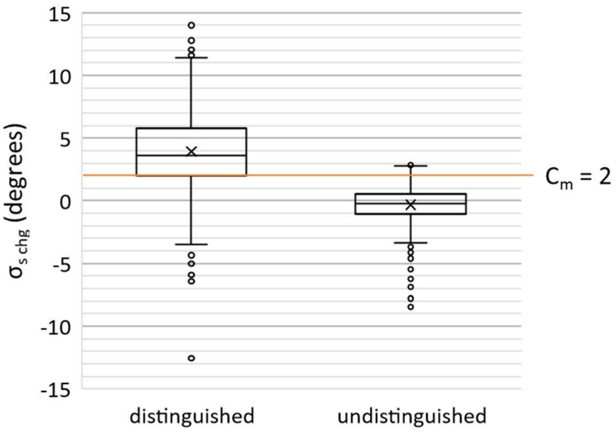

Figure 2. Box plots of $\sigma_{s\,chg}$ for the locations with cracks distinguished and undistinguished. The interquartile range is represented by the box. Upper whiskers: 1.5 times the interquartile range above the third quartile. Lower whiskers: 1.5 times the interquartile range below the first quartile. Outliers are plotted as dots. The horizontal line represents the median value of $\sigma_{s\,chg}$.

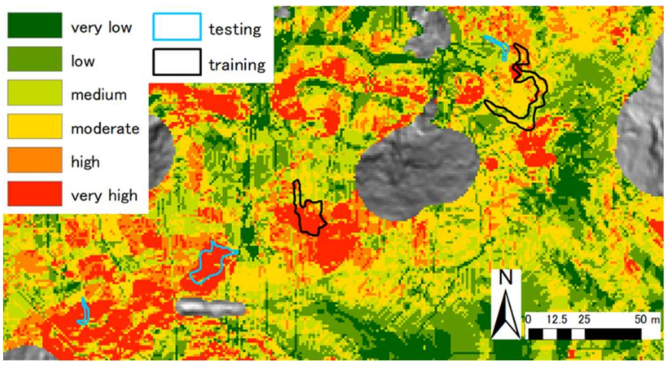

Figure 3. A part of susceptibility map for post-seismic slides. Areas of co-seismic slides were omitted from the analysis. Susceptibility is categorized into 5 classes, very high (10%), high (10%), moderate (20%), medium (20%), low (20%) and very low (20%).

1.03 to 1.13, confirming their independence. *C* values obtained for each conditioning factor were summed for each 1-m cell and used as a landslide susceptibility index for the cell. The accuracy of the models with/without use of the DCI was compared based on the area under the receiver operating characteristic curve (AUC) for true and false positive rates.

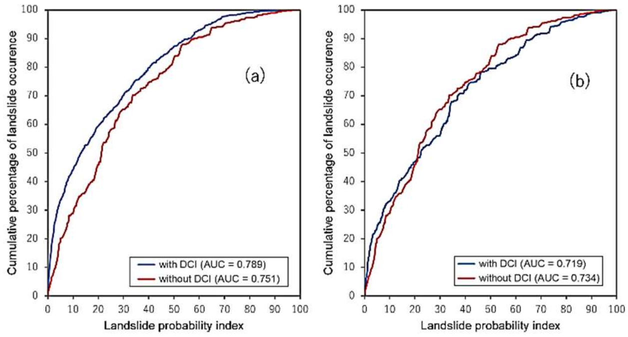

Figure 4. ROC curves calculated for (a) training and (b) testing slides.

IV. Results and Discussion

The standard deviation of slope angle increased by more than 2° after the earthquake in 75% of the locations where ground cracks were identified; therefore, we set C_m as 2° (Figure 2). Table 1 shows a negative contrast for DCI values < 0.2, which increased in classes with high DCI values. Overall, the factor that had the greatest influence on post-seismic slides was a DCI value over 0.6. The results suggest that integration of the DCI was favorable for estimating susceptibility to post-seismic landslides. Profile curvatures from -4 to 0, which corresponded to knick lines, and slope angles from 35° to 50° were other topographic features closely associated with landslide occurrence; this finding was consistent with a previous field investigation of post-seismic landslides in the same region [6]. A profile curvature < -4 corresponded to abrupt profile changes, such as cliff tops. Positive contrasts for the 0–4 plan curvature classes demonstrated concave slopes where landslides were likely to occur, whereas those > 4 mainly indicated narrow ridges.

Part of a post-seismic-slide susceptibility map is presented as an example in Figure 3. When using the DCI, the AUC values for training and testing slides were 0.79 and 0.72, respectively (Figure 4), which were within the range considered acceptable by the model [10]. In contrast, the AUC values for cases without DCI were 0.75 for training slides and 0.73 for testing slides (Figure 4). We obtained a slight improvement in the training data, but no improvement in the testing data upon incorporating DCI, despite the close association of the index with landslide occurrence (Table 1). This result can be partly explained by the manner in which the topographic features were represented by conditioning factors, and also by deficits in the bivariate model, which did not consider associations among controlling factors. In addition, a small number of landslide data, particularly in the testing dataset, disproportionately affected the modelling results. Further study using larger datasets is required to find the most appropriate combination of topographic factors and statistical model to increase the accuracy of post-seismic slide susceptibility assessments. Tectonic, seismic, lithological, climatic, and vegetation conditions should also be considered to extend the applicability of the model and help to prevent disasters caused by post-seismic landslides during restoration work undertaken after powerful earthquakes.

Table 1. Contrast for conditioning factors.

Conditioning factor	class	W^+	W^-	contrast
DCI	－0.2	-0.440	0.673	-1.113
	0.2－0.4	0.499	-0.193	0.692
	0.4－0.6	0.968	-0.090	1.057
	0.6－	1.899	-0.041	1.940
Slope angle (degree)	－20	-2.184	0.098	-2.283
	20－25	-1.503	0.067	-1.570
	25－30	-0.696	0.066	-0.762
	30－35	-0.075	0.013	-0.089
	35－40	0.329	-0.091	0.420
	40－45	0.568	-0.146	0.714
	45－50	0.371	-0.047	0.418
	50－	-0.005	0.001	-0.005
Plan curvature	－-4	-1.760	0.074	-1.835
	-4－-2	0.032	-0.004	0.036
	-2－0	-0.261	0.082	-0.342
	0－2	0.320	-0.193	0.513
	2－4	0.326	-0.056	0.382
	4－	-0.520	0.041	-0.561
Profile curvature	－-4	-1.252	0.036	-1.289
	-4－-2	0.469	-0.060	0.528
	-2－0	0.449	-0.387	0.835
	0－2	-0.424	0.193	-0.617
	2－	-1.422	0.098	-1.520
TWI	－2	0.050	-0.042	0.091
	2－4	-0.059	0.034	-0.092
	4－6	0.236	-0.042	0.277
	6－	-1.378	0.038	-1.415

REFERENCES

[1] Van Westen, C.J., N. Rengers, R. Soeters, 2003. “Use of geomorphological information in indirect landslide susceptibility assessment”. Nat. Hazards 30, 399-419.

[2] Reichenbach, P., M. Rossi, B.D. Malamud, M. Mihir, F. Guzzetti, 2018. “A review of statistically-based landslide susceptibility models”. Earth Sci Rev 180, 60-91.

[3] Tanyaş, H., M. Rossi, M. Alvioli, C.J. van Westen, I. Marchesini, 2019. “A global slope unit-based method for the near real-time prediction of earthquake-induced landslides”. Geomorphology 327, 126-146.

[4] Tanyaş, H., C.J. van Westen, C. Persello, M. Alvioli, 2019. “Rapid prediction of the magnitude scale of landslide events triggered by an earthquake”. Landslides 16, 661-676.

[5] Nowicki Jessee, M.A., M.W. Hamburger, K. Allstadt, D.J. Wald, S.M. Robeson, H. Tanyaş, M. Hearne, E.M. Thompson, 2018. “A global empirical model for near-real-time assessment of seismically induced landslides”. J. Geophys. Res. Earth Surf. 123-8, 1835-1859.

[6] Committee for Seismic Crack Counterplan in the Tateno District, 2019. “Field Investigation Report”. Kumamoto Prefecture.

[7] Bonham-Carter, G.F., 1994. “Tools for Map Analysis: Multiple Maps”. Geographic Information Systems for Geoscientists: Modelling with GIS, Pergamon (Elsevier Science Ltd), pp. 267-338.

[8] Frankel, K.L., and J.F. Dolan, 2007. “Characterizing arid region alluvial fan surface roughness with airborne laser swath mapping digital topographic data”. J. Geophys. Res. Earth Surf. 112, F02025.

[9] Toda, K., 2012. "Development of the microtopographical map by using airborne LIDAR DEM". J. Jpn. Soc. Erosion Control Eng. 65-2, 51-55.

[10] Hosmer, D.W., and S. Lemeshow, 2000. “Assessing the Fit of the Model”. Applied Logistic Regression, John Wiley and Sons, Inc., pp. 143 -202.